CASE STUDY
RELIABILITY IMPROVEMENT PROJECT
MULTI-STAGE FABRICATED CENTRIFUGAL BLOWERS

Ken Singleton
Manager, KSC Consulting LLC
19676 Serenity Lane
Bristol VA 24202
ksingleton@vibrationconsulting.com

Steve Quillen
Engineering Technologist
Eastman Chemical Company
Kingsport TN 37602
squillen@eastman.com

Abstract: Multistage fabricated centrifugal blowers are used by many companies for relatively low cost air and gas service. A popular model has impellers mounted on a shaft supported at both ends by ball bearings and direct coupled to a motor. This article discusses the in-depth analysis of six blowers and efforts to reduce maintenance costs and improve reliability. Vibration analysis, transient vibration data captured during startup and coastdown, operating deflection shape analysis, experimental modal analysis, rotor dynamic models, continuous laser alignment measurements, witnessed shop disassembly, balancing and reassembly were used to provide an understanding of the dynamics of the blowers, pipe strain effects on alignment and help identity improvement opportunities to increase reliability.

Key Words: Centrifugal blower, experimental modal analysis, flexible rotor balancing, misalignment, operating deflection shape analysis, rotor-bearing dynamic model, pipe strain, structural resonance, transient vibration data.

Background: Six multi-stage fabricated centrifugal blowers were used to convey gas with high levels of acetic acid, see **Figures 1-3**. The construction of the blowers required stainless steel for the shaft, impellers, hubs and housing. Each blower and motor was bolted to a stainless steel frame which was supported on one inch thick cork isolation material. Flexible bellows of stainless steel were used at the inlet and discharge flanges with the intent to eliminate pipe strain.

Specifications for the six blowers were as follows:

A. Blowers: 1500 ICFM, 150 Deg F Inlet Temp, Inlet Pressure 14.05 psia, Differential Pressure 10.0 psig, Discharge Pressure 24.5 psig, Specific Gravity 1.0, 125 HP, 3575 RPM, Direct Drive, Altra-Flex Couplings.
B. Motor: 125 HP, 460 V, 143 Amp, 3563 RPM, Frame 444TS, Wt 1650 lb.

The blowers typically operated 12 to 18 months between failures rather than the expected five years. Bearing failures were the most common reported problem.

Figure 1. Photo of Multi-Stage Centrifugal Blowers.

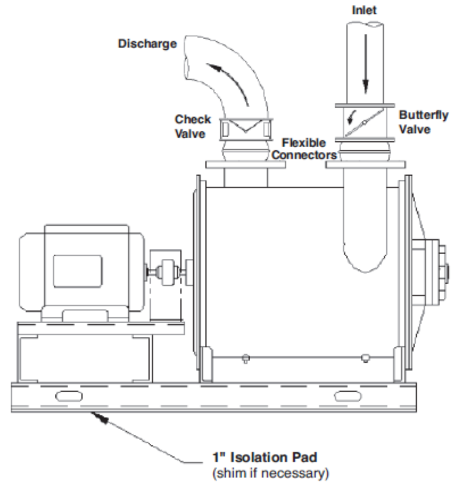

Figure 2. Showing Piping Connections and 1" Isolation Pad Under Skid.

Typical Multi-Stage Centrifugal Blower, Direct Drive

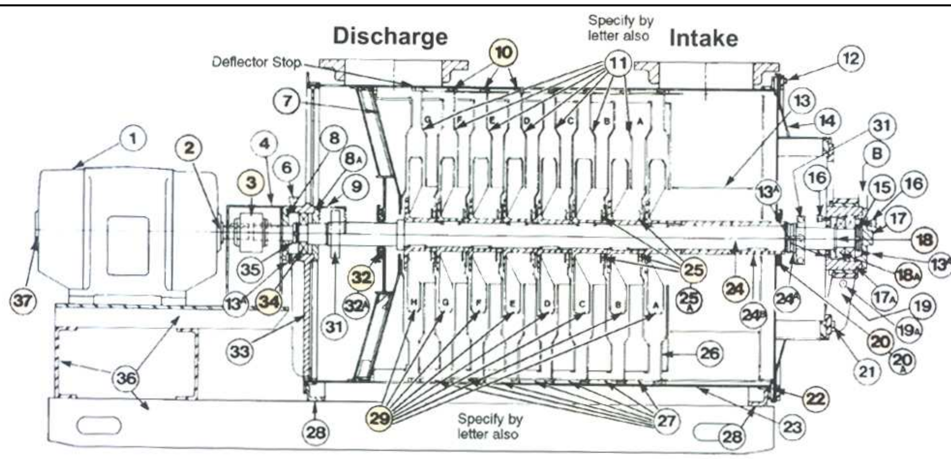

Figure 3. Schematic of Fabricated Centrifugal Blower.

Theory of Operation: A typical multi-stage centrifugal compressor is shown in **Figure 3**. The flow approaches the impeller through the blower inlet duct in an axial inward direction. A low pressure region is created by the impeller at the inlet face or eye of the impeller. The flow then enters the rotating impeller and is drawn through the impeller. The kinetic energy associated with the inlet relative flow may equal to 20% - 40% of the total work input.

The flow is then propelled through the impeller with work being continuously transferred to the flow as it transits through the impeller passages. The impeller is responsible for the work input and the resulting pressure which is related to the rotational speed. As the flow exits the impeller, it moves in a highly

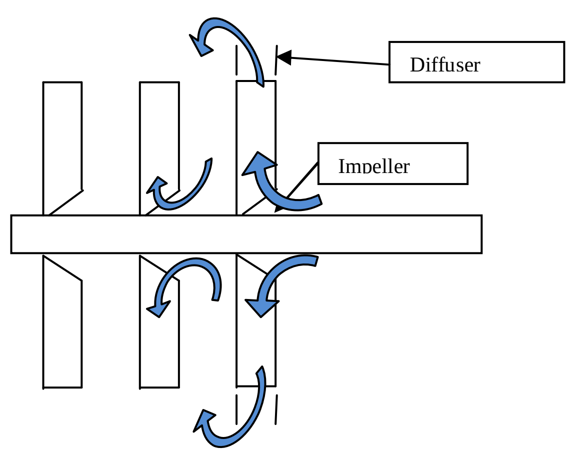

Figure 3. Schematic of Rotor With Impellers Showing Gas Flow.

tangential direction, not a radial direction, with a relatively small radial component. The kinetic energy level is very high which is required if any reasonable pressure rise or work input is be achieved. Approximately 2/3's of the pressure rise occurs in the impeller and an additional 1/3 in the diffuser. Depending on the design, anywhere from 50% to 70% of the kinetic energy leaving the impeller may be recovered as a static pressure rise in the diffuser.

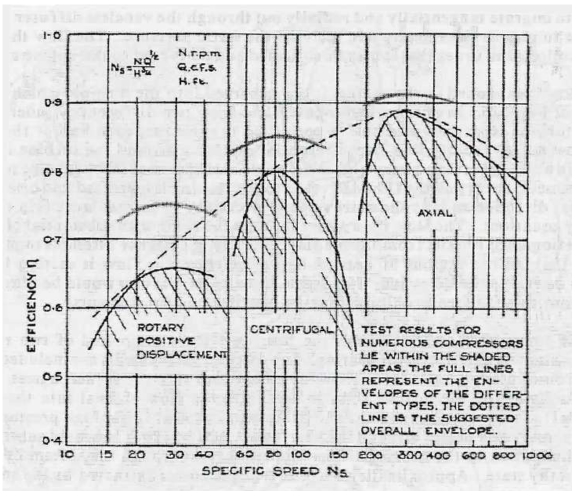

Figure 4. Variation of Efficiency With Specific Speed For Three Types of Compressors. [Ref 5]

A comparison of flow levels through rotary positive displacement, centrifugal, and axial compressors is shown in **Figure 4**. This chart is intended to provide a very simple representation and according to the author in Ref 5, only serves to illustrate a facet of machinery efficiency characteristics.

Periodic Vibration Analysis: Periodic vibration monitoring had shown high amplitudes of vibration primarily at 1X and 2X the run speed frequency of the motors and blowers.

At the beginning of the project, the most recent data for overall vibration in/sec pk were reviewed are shown in **Figure 5** for the six motor-blowers. Vibration limits are per ISO 10816-3 Machinery Group 2 & 4, Flexible Mount.

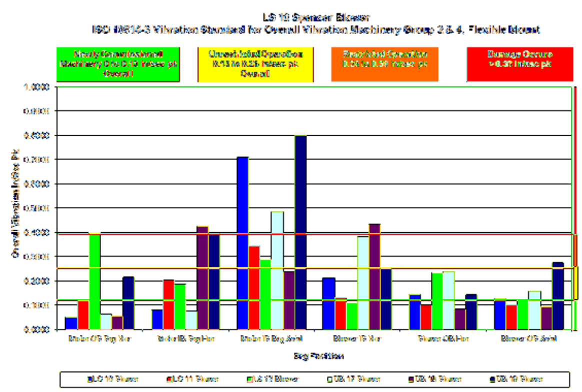

Figure 5. Periodic Vibration Monitoring Overall Data. Vibration Limits Per ISO 10816-3 Group 2 & 4, Flexible Mount.

Note that no vertical measurements were taken on the motor or blower bearing housings. These data showed that the location of highest amplitude vibration on all units was the Motor Inboard Bearing Axial direction. Blower DB18 had motor axial vibration of 0.80 in/sec pk. The high amplitude axial motor vibration was an indicator that the motor had a rocking motion. This was confirmed when additional data points were measured for the operating deflection shape analysis (ODS).

The blower OEM's published vibration limits were 0.275 in/sec pk which is slightly higher than ISO's Unrestricted Operation Limit. As shown by the chart, **Figure 5**, there were many points exceeding this limit.

A frequency spectrum and time waveform for DB 19 Blower Motor IB Brg Axial is shown in **Figure 6**. Most vibration energy was 1X the motor run speed frequency which could indicate unbalance, misalignment, resonance, bowed rotor, worn bearings, etc. The spectrum and waveform data alone were not sufficient to diagnose the cause of the high vibration.

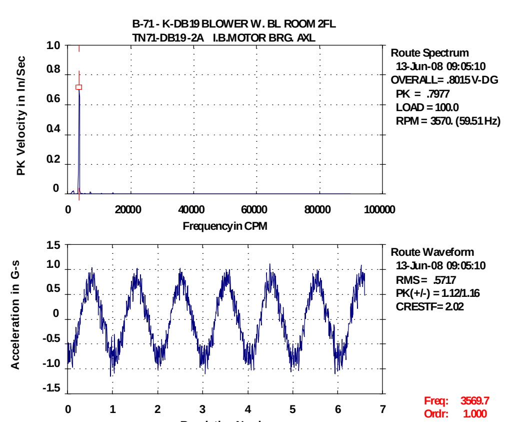

Figure 6. Frequency Spectrum and Time Waveform, DB 19, Motor IB Brg Axial.

The bearings in the motors and blowers were as follows:

- Motor – 6314 ball
- Blower Inboard – 6313 ball
- Blower Outboard – 7313 double row angular contact ball

Bearing defect frequencies and indications of lack of lubrication were identified in some of the vibration data measured on the bearing housings of the motors and blowers.

Operating Deflection Shape Analysis: Operating Deflection Shape Analysis (ODS) provides a 3D computer model of a machine or structure that can be animated at the various frequencies that vibration is occurring. The vibration shape or pattern can be studied at any of the frequencies measured by the cross channel transmissibility data.

The ODS 3D models for blowers DB 17, DB 19 and LS 10 were developed in ME'scopeVES V5.0 software. Cross channel transmissibility data was acquired with a 2 channel CSI 2120 spectrum analyzer on each blower. The data were measured by attaching a reference accelerometer to the blower outboard bearing housing in the horizontal direction and taking measurements with a second accelerometer at various locations on the motor, blower and skid frame. The data was uploaded from the analyzer to AMS Asset Management software then exported to ME'scopeVES and mapped to the 3D models to generate the animations.

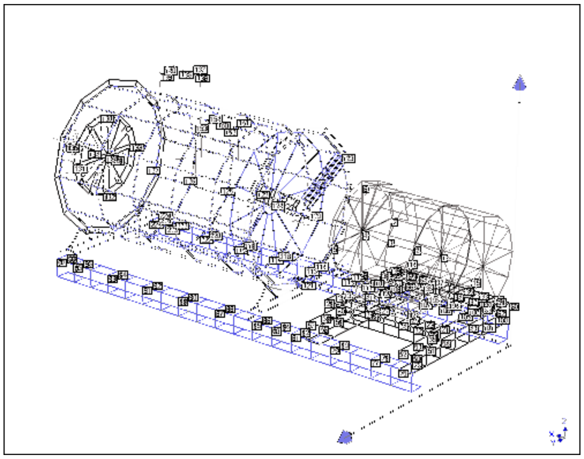

Figure 7. Wire Frame Model of a Motor, Blower and Skid With Measurement Point Locations Labeled.

Measurement point locations are shown in **Figure 7**. Data was measured in the X, Y and Z directions at each point unless access was limited. Interpolation was used to calculate the movement at unmeasured points based on a weighted calculation of the vibration at the nearest measured points.

ODS DB 19 Blower: The ODS model for DB 19 Blower 1X run speed with some data points labeled is shown in **Figure 8**. Very high amplitude vibration was measured on the motor in the axial, vertical and horizontal directions. Axial vibration measured 1.073 in/sec pk on the motor feet and 1.179 in/sec pk on the frame supporting the motor. The blower frame vibration also had high amplitude vibration at most points (two points are labeled in **Figure 8**).

The animation of the ODS model showed flexing of the frame and out of phase movement of the motor relative to the blower inboard bearing housing. The motor and supporting frame also had a rocking motion in the vertical direction and flexure of the frame.

The spectrum shown in **Figure 9** with log magnitude scaling was measured at the motor inboard bearing housing in the horizontal direction. It showed indication of a structural resonance just above the run speed frequency.

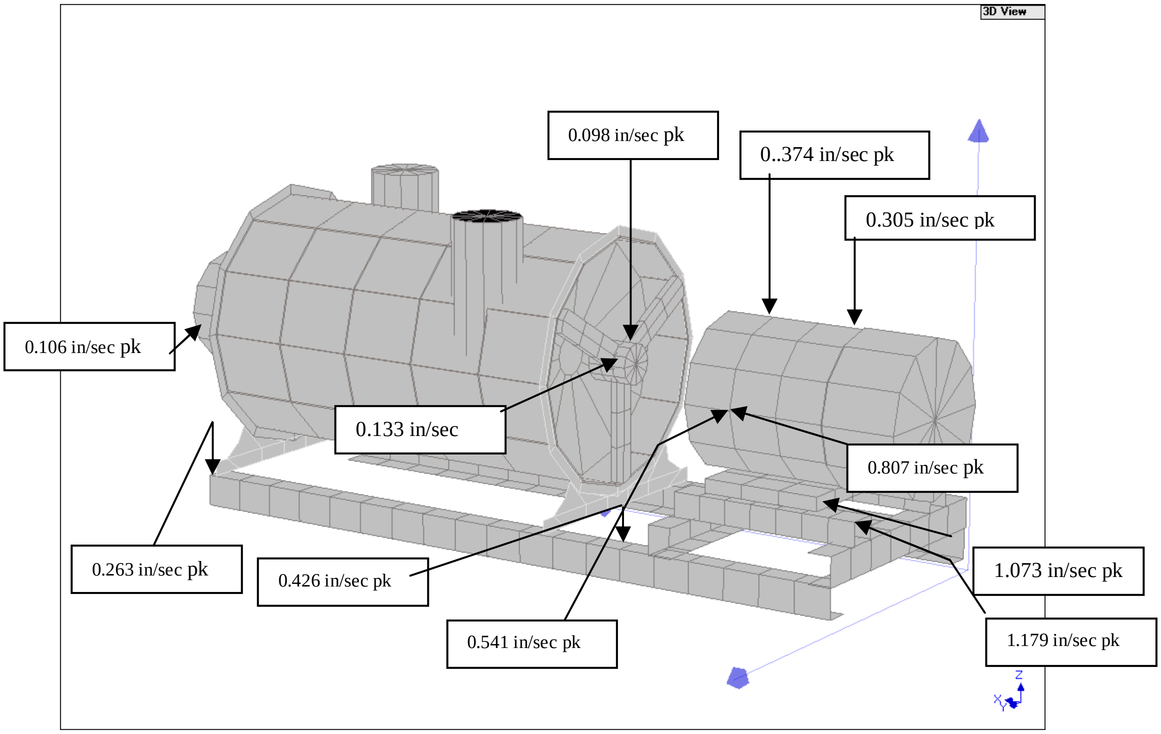

Figure 8. DB 19 ODS Vibration Amplitudes at 1X Run Speed Frequency.

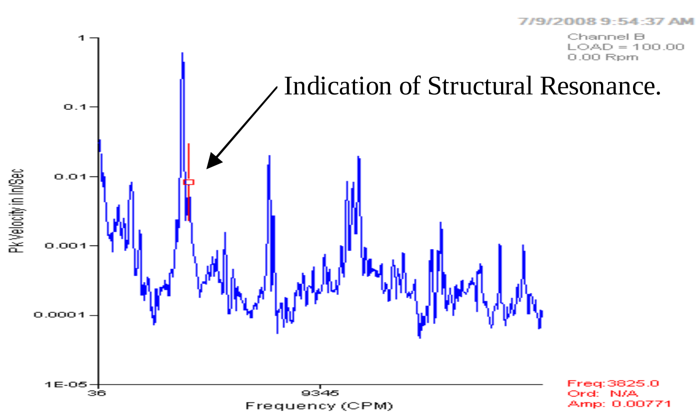

Figure 9. Spectrum (Log Mag Scaling) at DB 19 Motor IB Brg

Vibration amplitudes at 2X the run speed frequency of DB 19 were relatively low.

ODS LS 10 Blower: The ODS vibration data showed high amplitude vibration of the motor in the axial direction and vertically at the drive end. Vibration amplitudes were low at 2X the running speed frequency. Some flexure and bouncing of the skid on the cork was evident but amplitudes were not excessive.

ODS DB 17 Blower: The ODS vibration data showed high amplitude vibration of the motor with a rocking motion in the axial and vertical direction. The outboard blower bearing had very high amplitude vibration in the vertical direction. Flexure of the skid was very evident. DB 17 vibration amplitudes were low at 2X the running speed frequency. Some flexure and bouncing of the skid on the cork was evident but amplitudes were not excessive.

Pipe Strain: Inlet and discharge piping were connected to the blower nozzles using flexible stainless steel bellows. Tie bolts had been added using lugs welded to the flanges of some bellows as shown in **Figures 10 & 11**. Note that the bellows are completely compressed axially.

The piping was supported by hangers but not restrained at the blowers to prevent excessive pipe strain on the blower nozzles during thermal growth of the piping, see **Figure 12**.

Bellows expansion joints can accommodate small amounts of axial and lateral movement. They are not designed to compensate for piping misalignment errors. Pipe guides should be installed within four diameters of the joint and then again after fourteen pipe diameters.[Ref 6] The inlet and discharge piping to the blowers was not restrained so the bellows were transferring pipe movement forces to the blower nozzle flanges.

Figure 10. LS 12 Blower, Compressed Bellows at Intake Nozzle.

Figure 11. Blower LS 10 Blower Discharge Connection, Bellows Collapsed.

Pipe Hanger

Figure 12. Piping Connected to Blowers, Blower DB 19 Shown.

Continuous Vibration Acquisition: A multi-channel IOtech 618 Analyzer and eZ-Tomas rotating machinery software was used to measure vibration data from accelerometers magnetically attached to Blower DB19. The blower was started and had such high vibration levels that the optical tachometer and the Permalign laser alignment equipment, shown in **Figure 13**, vibrated out of position. The blower was shutdown and restarted a few minutes later. The blower ran for almost two hours and was shutdown. The blower was restarted about 40 minutes later and ran for about 2 ½ hours, see **Figure 14**.

Each startup and coastdown exhibited very high amplitude vibration at the shaft rotational frequency. A resonance or a blower rotor critical speed at 2400 RPM was indicated by the spin up vibration data. The radial vibration response at each blower bearing was in phase in both the horizontal and vertical directions which is in agreement with a rotor 1st mode or 1st critical speed, see the bode' plot in **Figure 15,** blower inboard bearing housing. However, the blower OEM indicated that the rotor critical was about 1600 RPM and our rotor-bearing model (developed later) calculated to about 1660 RPM. A between-bearing rotor rub acting as a third bearing was suspected. This would explain the rotor critical moving higher in frequency.

Figure 13. DB 19 With Laser Alignment and Vibration Sensors Attached.

The amplitude of vibration during passage through the blower rotor critical reached extremely high amplitudes of over 6 in/sec pk at the inboard bearing housing as shown by the overall vibration trend plots in **Figure 14** and the bode' plot in **Figure 15**.

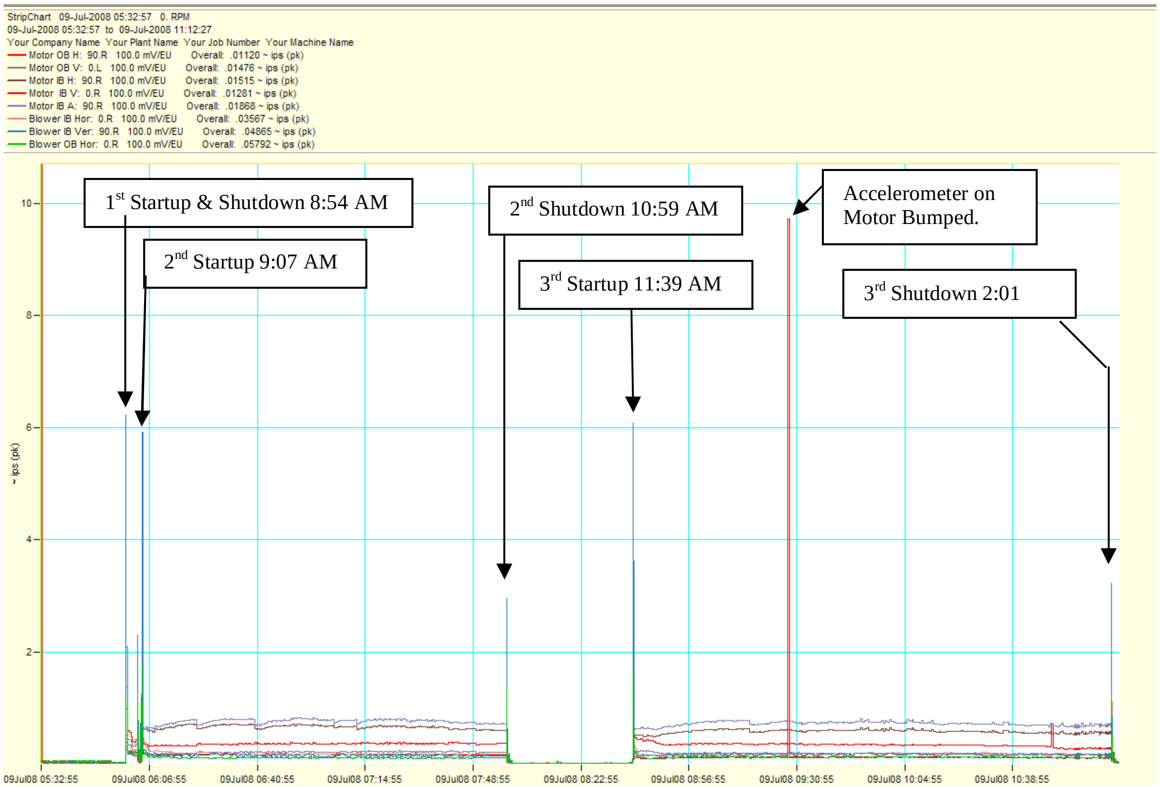

Figure 14. Overall Trend Vibration in/sec pk On DB 19 Blower, Channels 1 - 8.

The outboard bearing housing had much lower vibration and the critical speeds were lower at 2271 RPM during spinup and 2161 RPM during coastdown. The reason for this would not become apparent until the rotor model was analyzed with a rub condition at the packing location at the inboard end.

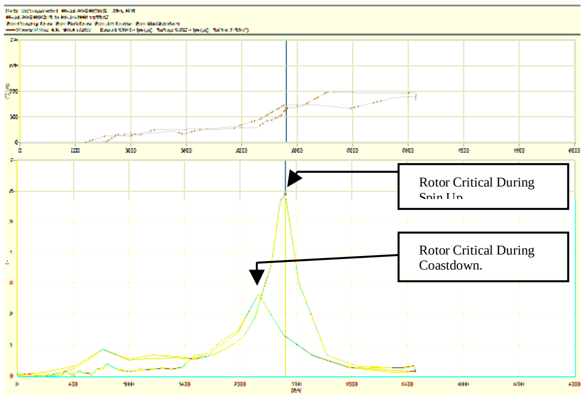

Figure 15: Bode' Plot of Blower IB Hor During 3rd Startup and Coastdown. Vibration Amplitude was Very High at About 5.9 in/sec pk.

Modal Test of Blower & Motor Mounted on Skid: An experimental modal test was conducted on a blower and motor mounted to a skid in the maintenance shop, **Figure 18**. The skid was supported on 1" thick cork to simulate the installed condition. A medium sledge modal hammer and CSI two channel 2120 analyzer were used to acquire the data.

A very responsive natural frequency was identified by the test data frequency response functions (FRF) at 43.5 Hz ~ 2610 CPM. As shown in **Figure 20** the run speed frequency of the motor-blower was within the envelope of the natural frequency which would result in amplification of vibration generated by unbalance and misalignment forces.

Figure 18: Blower & Skid Supported on Cork in the Maintenance Shop During Modal Test.

The mode shape of the natural frequency was bending of the skid rails in the vertical direction in the section between the motor support rails and the blower inboard feet mounting, see **Figure 19**. The natural frequency mode shape resulted in rocking of the motor vertically and axially. Excitation of this natural frequency was causing the very high amplitude motor vibration in the vertical and axial directions on the installed blowers.

Stiffening of the skid was recommended by welding ¼" plate about 55" long to the inside of both frame rails at the motor end, as shown in **Figure 21**. The intent was to box the frame rails increasing the moment of inertia in the Z axis (vertical direction). It was hoped that this would stiffen the rails enough to raise the natural frequency well above the running speed frequency. Plates welded on top of the rails in the locations shown would further

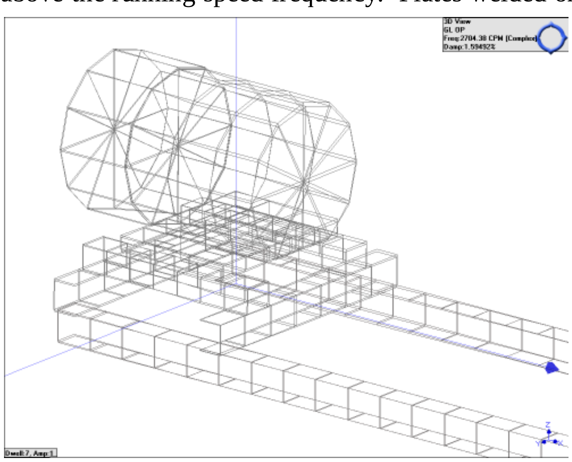

Figure 19: Animated Mode Shape of Rail & Motor Natural Frequency.

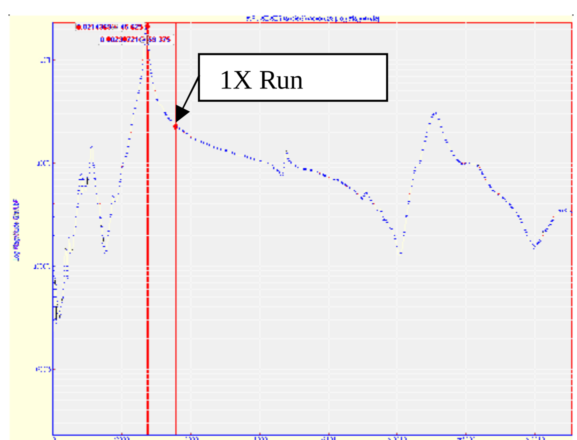

Figure 20: FRF on Motor IB Bearing Housing Showing Natural Frequency Near Running Speed.

increase stiffness in the Z axis at these locations if required. The decision was made not to modify the existing skid but to make those modifications to a new skid design to stiffen it in this area.

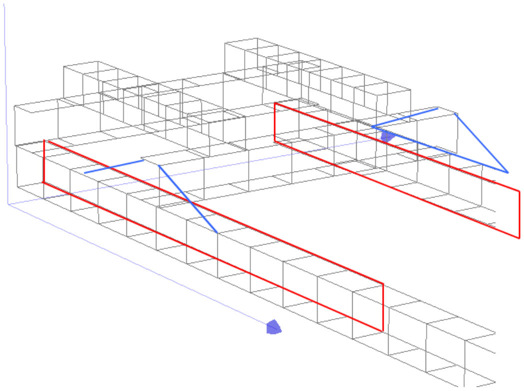

Figure 21: Suggested Stiffen Of the Skid Frame Rails Based on the Modal Test Results.

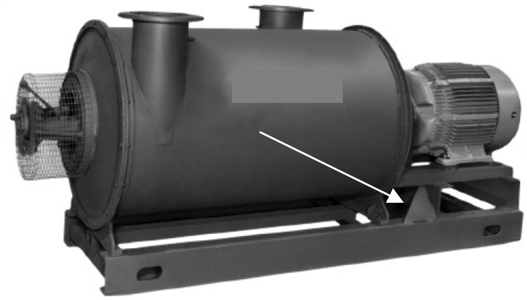

Figure 22. Stiffeners Originally Included in the Blower Design.

It would be discovered later that the blower OEM provided bolt-on stiffeners, as shown in **Figure 22**, but these stiffeners had been removed during maintenance for access to bolts. The stiffeners were not replaced.

Rotor Bearing Dynamic Analysis: A model of the blower rotor, **Figure 23**, was developed using DyRoBeS [Ref 4] finite element based software. The model included the dynamic mass and stiffness of the blower bearing housings measured by driving point impact modal testing. The impellers were weighed and the transverse and polar moments of inertia calculated. Stiffness of the ball bearings was calculated using a DyRoBeS utility. Note that the 1^{st} four impellers are larger diameter. Stages five through ten have smaller diameters.

The rotor bearing 1^{st} critical speed calculated to 1660 RPM, see **Figure 24**. Potential energy distribution, **Figure 25**, showed that the stiffness of the shaft was primarily controlling response at the 1^{st} mode. The bearings calculated to have less than 1% of the potential energy which is well below the 20% recommended by Dr Gunter.[Ref 2] This meant that the bearings would not contribute to the overall system damping; the rotor would be very sensitive to unbalance and high vibration at the 1^{st} critical would expected.

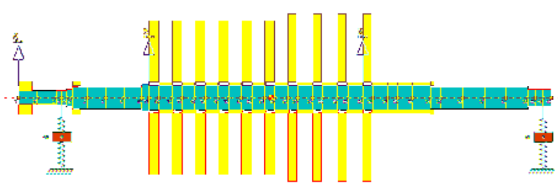

Figure 23. DyRoBeS [Ref 4] Blower Rotor-Bearing-Support Model.

Maximum dynamic stress in bending at the 1^{st} critical calculated to 881 psi, **Figure 26**, which was not a concern. The nodal points of the 1^{st} mode were located approximately 4 inches outside each bearing.

In **Figure 27**, is a 3D plot of the rotor response at the 1^{st} mode to unbalance of 2.872 oz-in (G 6.3) in Impeller 10 and 2.203 oz-in in Impeller 1. Maximum shaft displacement mid-span for this unbalance calculated to about 11 mils p-p. The unbalance force at the bearings calculated to 184 lb_f at the drive end bearing and 157 lb_f at the opposite drive end bearing.

A rule of thumb for flexible rotor design is the 10:1 rule, i.e., the shaft diameter should not be less than 1/10 the bearing span. This design calculated to just over 20:1 which explains the high response at the 1^{st} critical speed since the stiffness of the shaft, which is low due to the long span, offers the primary resistance to the unbalance force.

The damped unbalance response at the bearings for G6.3 unbalance in the 1st and 10th stage impellers is plotted in Bode' format in **Figures 28 & 29**.

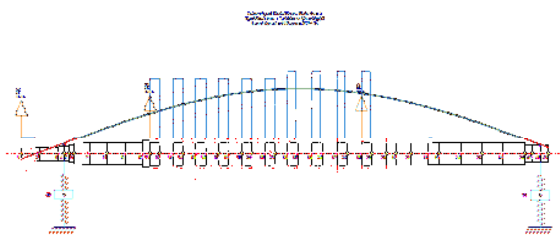

Figure 24. Rotor 1st Mode. Nodal Points are About 4" Outside Each Bearing.

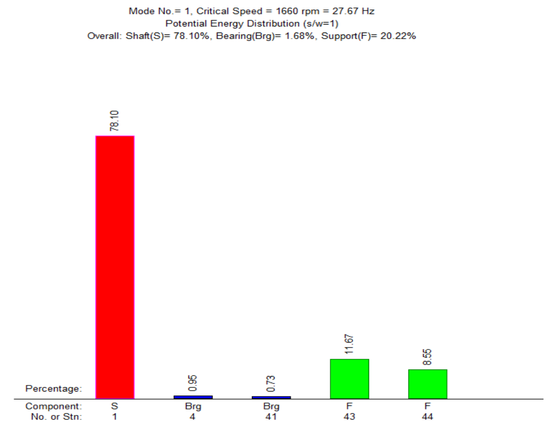

Figure 25. Potential Energy Distribution Showing Most Energy in the Shaft but the

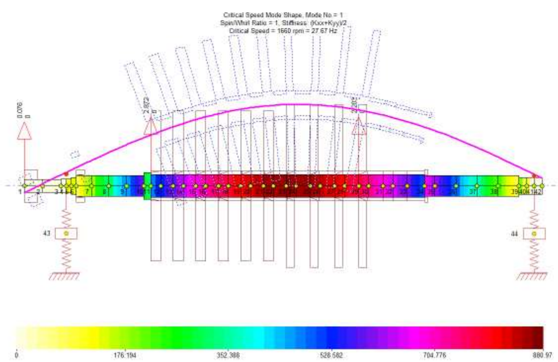

Figure 26. Maximum Dynamic Stress in Bending at 1st Mode Calculated to 881 psi.

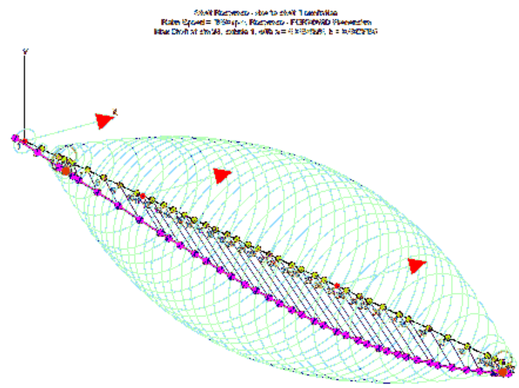

Figure 27: Rotor Response at 1st Critical to G 6.3 Unbalance in the 1st and 10th Stage Impellers. Maximum Orbit Mid-Span Calculated to About 11 mils pp.

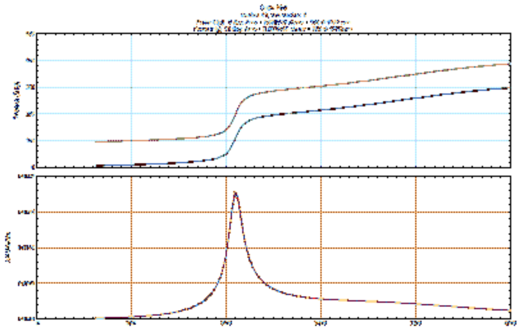

Figure 28. Bode' Plot of Damped Unbalanced Response at the Opposite Drive End Bearing to G6.3 Unbalance in 1st and 10th Stage Impellers.

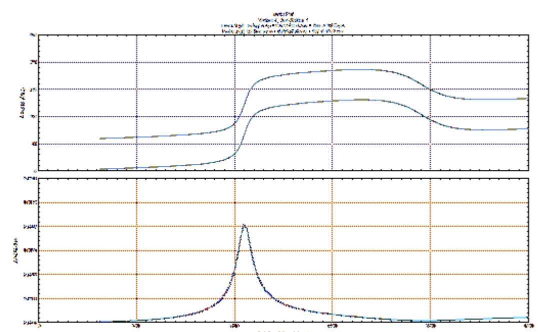

Figure 29. Bode' Plot of Damped Unbalanced Response at the Drive End Bearing to G6.3 Unbalance in 1st and 10th Stage Impellers.

Simulation of Rub: The spin up and coastdown data on DB 19 Blower had showed very high amplitude vibration at about 6.0 in/sec pk at the 1st critical speed of 2400 RPM (spin up) and 2160 RPM (coast down). These critical speeds were higher than our rotor model predicted and also higher than the OEM had predicted which was 1600 RPM.

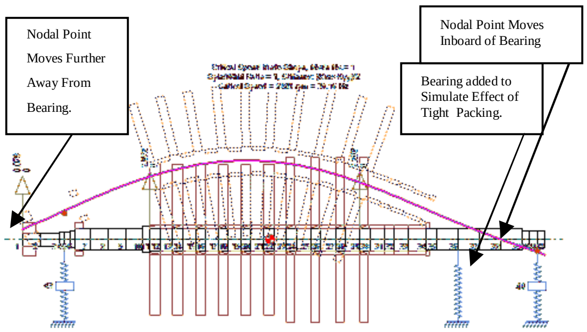

Figure 30. Spencer Blower Rotor Model with Bearing Added at the Packing Location to Simulate the Stiffening Effect of the Packing.

A third bearing was added to the DyRoBeS model at the packing location, station 36. The packing location was the only location identified at disassembly where significant contact with the shaft by a non-rotating component had occurred. Trying different values of stiffness it was found that 200,000 lb_f/in at the packing location calculated to raise the critical to about 2289 RPM as shown in **Figure 30**. Note that the mode nodal point then moves inboard of the opposite drive end bearing while the nodal point moves further away from the drive end bearing. Therefore, higher vibration would be expected at the drive end bearing (which was measured) than at the outboard bearing housing.

Strain energy distribution is shown in **Figure 31 & 32** with and without the packing acting as a bearing. The model predicted that the packing would see significant strain energy and also an increase in strain energy at the inboard bearing housing. This is in agreement with the vibration data which measured very high response at the inboard bearing housing.

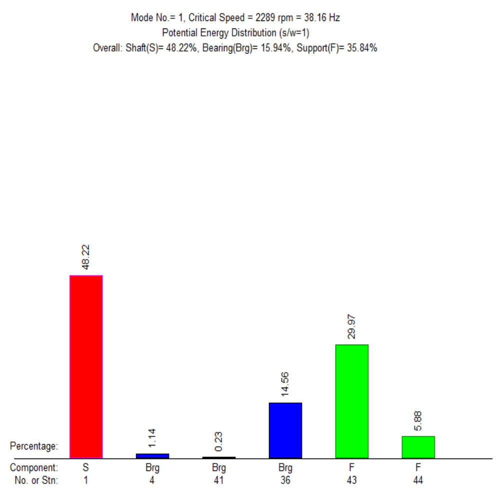

Figure 31. Comparison of Strain Energy Distribution With Packing Acting as a Bearing.

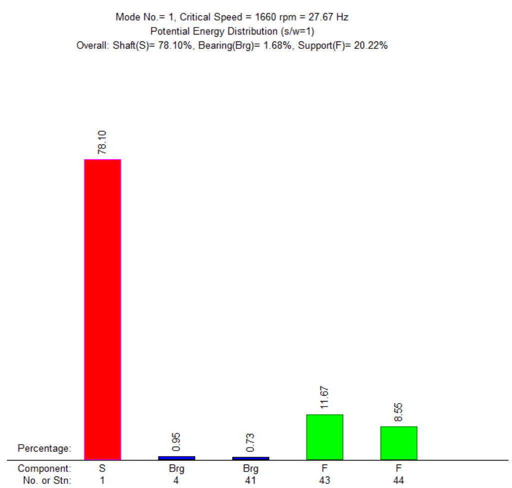

Figure 32. Comparison of Strain Energy Distribution Without Packing Acting as a Bearing.

The damped unbalanced response at the bearings and mid-span of the rotor with the packing preload is shown in the overlaid plot in **Figure 33**. The maximum displacement at the mid-span stations calculated to about 11.5 mil pp at stations 22-24 at 2400 RPM.

Based on the results of the rotor-bearing models, very careful attention to rotor machining tolerances, assembly and balancing would be required to achieve acceptable vibration levels through the critical speed region. The design uses a metal-to-metal interference fit of the impeller hubs to the shaft. After the rotor is balanced, it is disassembled. Then the rotor must be reassembled in the case and there is no opportunity to test or change the balance as each impeller is reinstalled on the shaft.

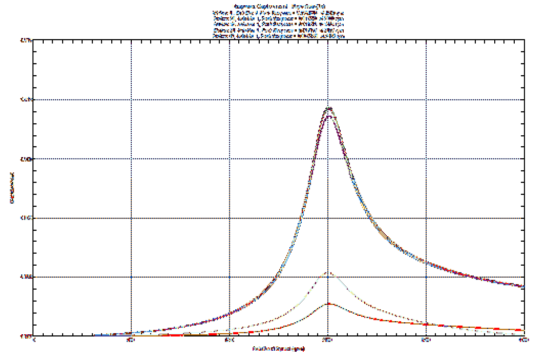

Figure 33. Damped Unbalanced Response for Several Locations With Packing Rub Affect.

Frequency spectra are plotted in **Figures 34-A thru 34-F** that were measured on the Inboard Bearing Housing, Horizontal, during the 3rd startup of Blower DB 19. The spectra show the 1st critical shifting higher in frequency as the rotor bows out and rubs against the packing harder. Once the rotor is at speed and well above the rub affected critical, the 1st critical dropped to about 1425 CPM. This is lower than the calculated frequency of 1675 CPM. However, it was learned when the blower was disassembled that the shaft bearing fits were undersize and the bearing housing bores oversize. These increased clearances would lower the support stiffness thus lowering the 1st critical speed about 250 CPM from "as new" condition.

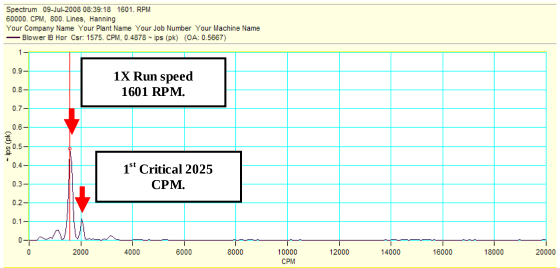

Figure 34-A. Blower DB 19, 3rd Startup, Frequency Spectrum at 1601 RPM.

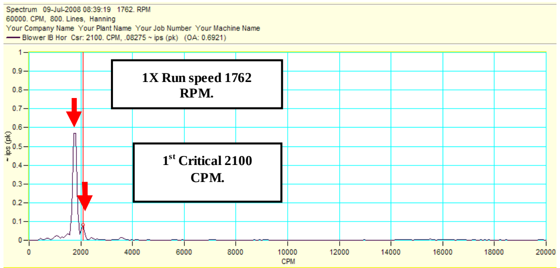

Figure 34-B. Blower DB 19, 3rd Startup, Frequency Spectrum at 1762 RPM.

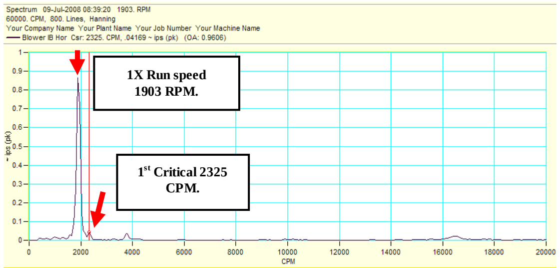

Figure 34-C. Blower DB 19, 3rd Startup, Frequency Spectrum at 1903 RPM.

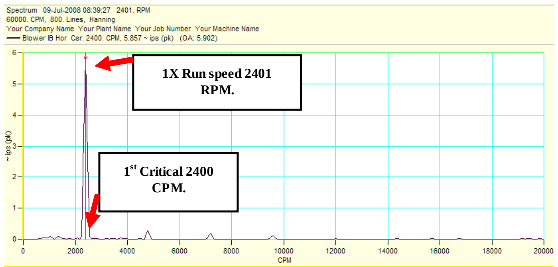

Figure 34-D. Blower DB 19, 3rd Startup, Frequency Spectrum at 2401 RPM.

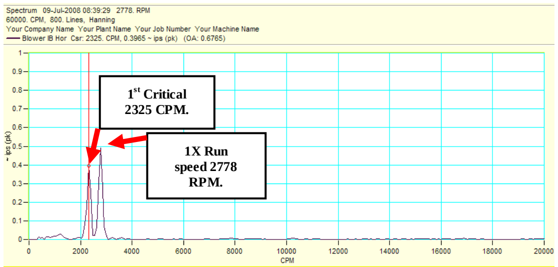

Figure 34-E. Blower DB 19, 3rd Startup, Frequency Spectrum at 2778 RPM.

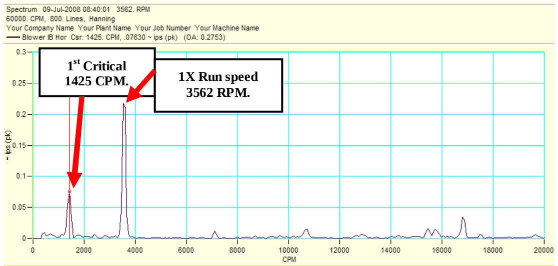

Figure 34-F. Blower DB 19, 3rd Startup, Frequency Spectrum at 3562 RPM.

Shaft Seals: Three seal options were offered by the blower OEM, 1) Packing Box, 2) Carbon Ring and 3) Mechanical Seal, **Figure 35**.

The packing box is the lowest cost but the packing rubbing the shaft causes heat, thermal bowing of the shaft and as calculations and vibration data indicated can shift the rotor critical speed much higher. Up to 30 mils shaft wear is allowed at the packing location per the blower OEM's manual. Packing was used on the six blowers in this analysis.

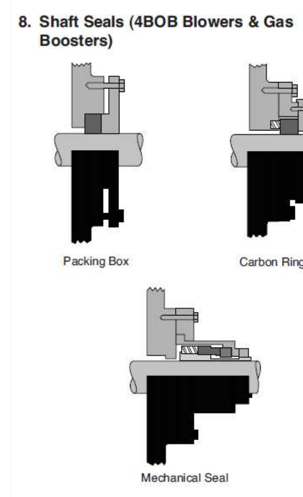

Figure 35. Seal Options Offered by Blower OEM.

Thermal Growth Measurements: A Ludeca Permalign [Ref 7] laser system was installed on blowers DB18 and DB19 as shown in **Figures 36 & 37**. The relative movement of the motors and blowers was measured as the units were started, came to operating temperature, shutdown and cooled to ambient temperature.

Figure 36. Laser Alignment Equipment, Ludica Permalign [Ref 7], Installed on the Motor and Blower.

Figure 37. Permalign [Ref 7] Setup on Blower and Motor.

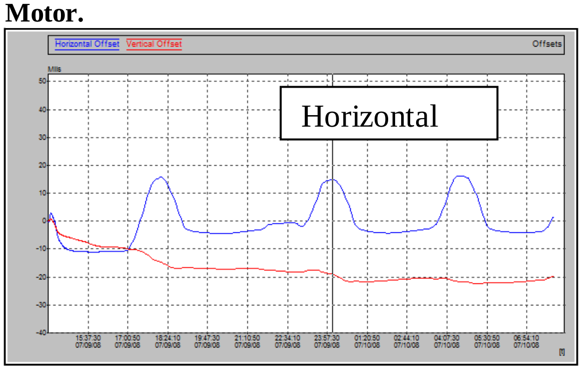

Figure 38. Blower DB19 Cool Down Alignment Data.

DB19 Blower was monitored first. The blower was shutdown and allowed to cool overnight. The Permalign was installed after shutdown. Data acquisition began the next morning. The blower was started and vibration became so severe (approximately 6.0 ips pk) that it vibrated the Permalign laser loose and also the accelerometers that were installed to monitor the run. The Blower was shutdown to allow re-adjustment of the Permalign Monitors and remount the accelerometers.

The blower was restarted two more time and finally allowed to run for about 2 ½ hours then was shutdown and allowed to cool down overnight back to ambient. Cool down data indicated severe pipe strain in the horizontal direction. The blower is being pushed/pulled. As shown by the data in **Figure 38**, there is a sudden horizontal movement about every 4-6 hours. This movement occurs when the other two blower are shutdown.

The data collection shown in **Figure 38** began just minutes before Blower DB19 was shutdown. Note that the blue line (horizontal offsets) jumps when the other two blowers are shutdown. The pipe strain forces the blowers out of alignment as much as 20 mils during each blower startup.

Coupling Targets for DB19

Note: All values are calculated at center of the coupling and should only be used at ambient.

Vertical Offset	Vertical Angularity	Horizontal Offset	Horizontal Angularity
-21 Mils	-2.5 Mils per 10" diameter	-4.1 Mils	-0.4 Mils per 10" diameter
Set Motor Low	Set gap on bottom (6:00)	Set motor west of blower	Set gap on west side (9:00)

Table 1. Alignment Targets for DB19. The Blower was Aligned to these Targets.

DB18 Cool Down Alignment File: The Permalign [Ref 7] was setup on this unit after DB 19 was re-aligned and started up. DB18 was started and allowed to reach operating temperature for about 5 hours then shutdown and allowed to cool overnight. The results were very similar to DB19 with the blower being pushed/pulled horizontally when the other two blowers shutdown as shown in **Figure 39**.

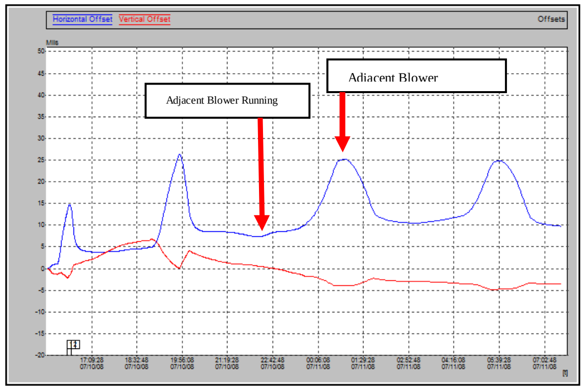

Figure 39. Permalign [Ref 7] Data File for DB18 Blower. Horizontal Movement Occurs When Adjacent Blower Shutdown.

Coupling Targets for DB18

Note: All values are calculated at center of the coupling and should only be used at ambient temperature.

Vertical Offset	Vertical Angularity	Horizontal Offset	Horizontal Angularity
-10 mils	-5.8 mils per 10" diameter	-4.5. Mils	+5.0 mils per 10" diameter
Set Motor Low	Set gap on bottom (6:00)	Set motor East of blower	Set gap on East side (3:00)

Table 2. Alignment Targets for DB18. The Blower was Aligned to these Targets.

Blower DB 19 Repair: DB 19 Blower was shipped to a Factory Authorized Service Center for disassembly, inspection, repairs, balancing, reassembly and run test. This process was witnessed by one of the authors.

The blower as received at the service center is shown in **Figure 40**. During disassembly, the 1st stage impeller is shown in **Figure 42**, before removal from the shaft.

The shaft is shown after unstacking, see **Figure 42**. There was excessive wear of the packing area, (greater than 30 mils wear).

Figure 40. Blower DB 19 As Received at Factory Authorized Repair Facility.

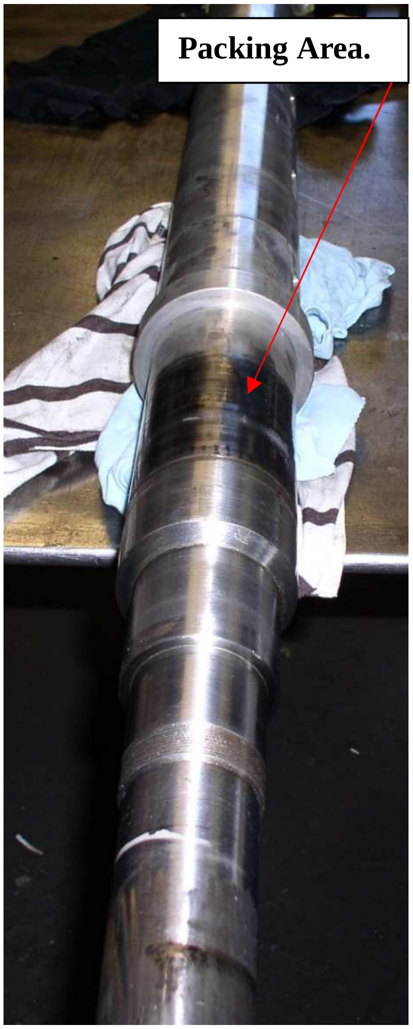

Figure 21.Shaft Packing Area Discolored by Packing Rubbing.

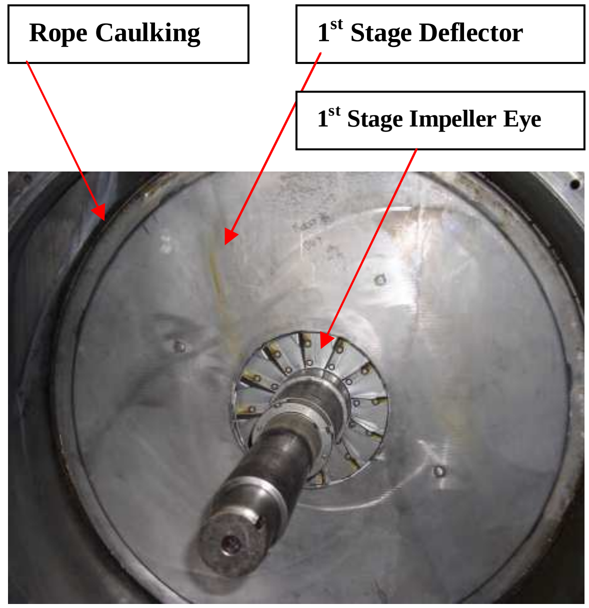

Figure 42. 1st Stage Impeller With Deflector and Rope Caulking at the OD.

Impeller #2 had minor blade damage, see **Figure 43**. The hub and blades showed heating from previous installation. Fretting corrosion was present in the hub bore indicating a loose fit on the shaft.

Keys were machined in an alternating manner on both sides of the shaft, see **Figure 44**. The keys in the shaft transferred torque to the impeller hubs.

Figure 43. Impeller #2 Blade Damage. Note Heating of the Hub Which Occurred During Previous Assembly.

Figure 44. Shaft Keyways Machined in Alternating Arrangement. Keys Transfer Torque to the Impeller Hubs.

the rotor being stacked for balancing and final rotor assembly on the balance machine is shown in **Figures 45-47**.

Figure 45. Impellers Being Installed on Shaft.

Figure 46. Bare Shaft in Balancing Machine. Impellers Are Stacked at the End of the Balance Machine.

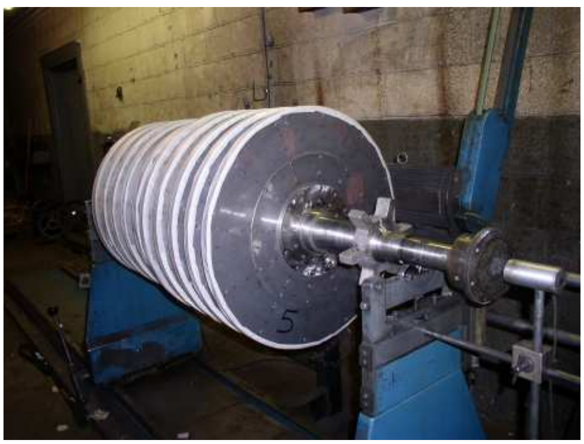

Figure 47. Rotor Stacked, Impellers Taped For Wind Resistance For Balancing.

Incoming Rotor Balance: The balance machine printout for the incoming and final balance are shown in **Figure 48**.

```
        Balance Report

Balance speed:  425  RPM            Balanced for Operating speed  3600  RPM

Half Key Weight:
   Near side      = 0 gm                  Far side      = 0 gm

Initial Unbalance
   Near Vibration:                       4.74 mils  at  276 degrees
   Near Velocity:                      0.105 in/sec
   Near Unbalance:                    10.1294 oz-in  or   287.1685 gm-in

   Far Vibration:                        4.19 mils  at  289 degrees
   Far Velocity:                       0.093 in/sec
   Far Unbalance:                     12.3922 oz-in  or   351.3191 gm-in

Finish Unbalance
   Near Vibration:                       0.48 mils  at    8 degrees
   Near Velocity:                      0.011 in/sec
   Near Unbalance:                     0.8950 oz-in  or    25.3737 gm-in

   Far Vibration:                        0.38 mils  at  188 degrees
   Far Velocity:                       0.009 in/sec
   Far Unbalance:                      0.7970 oz-in  or    22.5955 gm-in

Weight
   Near:           26.11 grams  or    0.92 ounces
   Far:            35.13 grams  or    1.24 ounces

ISO-1940 G 2.5 recommended maximum unbalance:  54.4733 gm-in
    Near side:  27.2367 gm-in    Far side:  27.2367 gm-in


weight 460 lbs shaft/10 impellers/spacers
]

(c) 2007 Dynamics Research Corp.
This unit has been precision balanced using our State-of-the-Art
Dynamics Research Corp. COMPUTER Balancer, United STATES PATENT NO.
5,627,762 + 5,412,583, AND OTHER PATENTS PENDING.
```

Figure 48. Service Shop Balance Report.

Using the data from the balance report, the forces generated by the rotor unbalance at each journal were calculated as shown in **Table 3**.

Incoming: Near Plane balance correction calculated to 233.0 lbf. Far Plane balance correction calculated to 212.4 lbf

After repairs and assembly, ISO G1.0 was met per the balance machine print out in **Figure 48**. Rotor runout measurements were not reported.

	Near Plane		Ubal Force lb_f	Far Plane		Ubal Force lb_f
Initial Unbalance	10.129	oz-in	233.017	12.392	oz-in	285.070
Finish Balance	0.895	oz-in	20.589	0.797	oz-in	18.334
Force Reduction			212.428			266.736
Percent Reduction			91.16%			93.57%
	grams	oz		grams	oz	
Correction Weight	0.89	0.03		2.26	0.08	
ISO G 1.0	19.184	gr-in	Near Side	9.592	gr-in	Far Side
	0.675	oz-in		0.338	oz-in	
	15.539	lbf		7.770	lbf	
Rotor Weight	450	lbf				

Table 3. Unbalance Forces For Incoming and Final Rotor Balance.

After balancing, the rotor was disassembled and reinstalled in the case. Heating of an impeller hub during reassembly using a torch is shown in **Figure 49**. Rope packing is installed between each stage to reduce leakage at the case/diffuser interface.

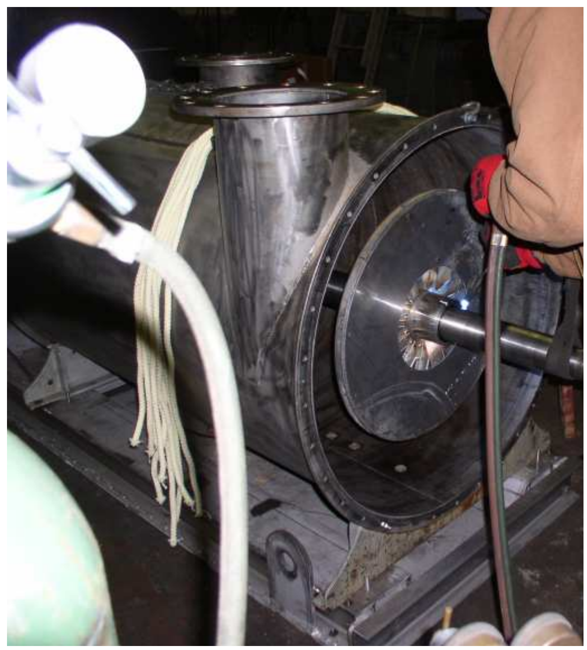

Figure 49. Reassembly. Torch Used to Heat Impeller Hub Prior to Sliding Into Position.

Conclusions:

- The design of the blower rotor was very flexible with a diameter to bearing span ratio of >20:1. The rotor lateral response was primarily controlled by the stiffness of the shaft which was relatively low due to the long bearing span. The bearings were located close to the 1st mode nodal points and provide little control of the 1st critical.

- Vibration amplitudes of the five blowers tested were well above industrial standards and guidelines published by the blower OEM.

- Vibration data on DB19 indicated unbalance of the blower rotating assembly and misalignment as the primary forcing functions. Unbalance was confirmed by balance machine measurements. The shaft fits were undersized at the bearings and more than 0.030 inch undersize at the packing fit. The shaft was replaced.

- Flexing of the skids (frames) supporting the motor and blower was clearly evident in the ODS models. The skid was redesigned by the equipment owner to improve support of the blower using thicker structural elements and additional stiffening and machining of mounting pads coplanar.

- The modal test of the blower and motor skid assembly showed a very responsive bending mode at the motor end of the frame within the operating speed range. The natural frequency mode shape resulted in a rocking motion of the motor in the vertical and axial directions. All five blowers tested had high amplitude motor vibration in the axial and vertical directions. It was discovered that stiffener plates/gussets originally provided by the OEM had been removed by maintenance personnel to gain access to hold down bolts but these gussets were not replaced.

- Inspection of the piping and bellows flexible connectors showed evidence of excessive pipe strain at the blower's inlet and discharge nozzles due to un-restrained thermal growth of the piping as the blowers cycled on and off. The piping was not adequately supported to prevent excessive pipe strain on the blower nozzles.

- Permalign data measured on DB18 and DB19 showed over 25 mils relative horizontal movement of the motor and blower during shutdown and cooling to ambient temperature. There were also excessive alignment changes when adjacent blowers cycled on and off caused by thermal growth of the piping pushing/pulling the blowers.

- DB 19 vibration test data showed extremely high amplitude vibration during startup and shutdown. A rotor 1st critical speed was indicated as high as 2400 RPM. Mid-span rub was suspected to act as a third bearing raising the rotor critical from about 1450 RPM to about 2400 RPM. Inspection of the rotor and rotor-bearing model confirmed that the packing was acting as a third bearing.

- Other options for sealing other than packing are available which include carbon ring and mechanical seal.

Recommendations:

The following recommendations were provided to plant management to improve reliability of the fabricated centrifugal blowers:

Blower overhaul, rotating assembly balancing and mechanical run test.
- Develop a rotor inspection process and inspection measurements.
- Rotor multi-plane dynamic balance of rotating assembly per ISO G1.0.
- Post overhaul, mechanical run test, 1 hour minimum after temperature stable.

Conduct Repair Facility Audit
- Incoming disassembly and inspection process
- Tolerance for replacement components
- Facility's Access to OEM drawings and specifications
- Assembly process – part inspection, shaft and impeller dimensions, allowable run out, balancing process, training of personnel, condition of measuring tools and machine tools
- Post overhaul run test capability

Modal test of first fabricated skid
- Ensure that no structural natural frequencies are within +/- 10% of 1X, 2X run speed.
- Modify skid design if test results indicate need.

Install permanent accelerometers on the Motor-Blower bearing housings
- Cable signals to switchboxes located outside the blower area. This addresses safety issues of accessing the blower inboard bearing housing and accurately measuring vibration of the motor bearing housing.
- Consider connecting accelerometers to IMI Model 682A05 Bearing Fault Detectors which can be monitored by PLC.

Blower Nozzle Loading (Pipe Strain)
- Piping study to determine piping thermal growth
- Recommendations for piping supports and flexible piping connections to the blower nozzles.
- Obtain allowable blower nozzle loading.

Actions Taken:

1. Witnessing of blower disassembly, repair, balancing, reassembly and run test at an authorized repair shop.

2. Plant management decision to begin overhauling the centrifugal blowers in-house. This would provide more control over dimensional accuracy of fits, balancing and assembly procedures.

3. Inspection form developed to document the blower shaft fit dimensions, fit runouts, impeller radial/axial runout.

4. The skid frame was redesigned using thicker elements and bracing. Blower mounting points were machined co-planer.

5. The cork under the skids was changed to meet the blower OEM's specifications.

6. A piping study was conducted. Supports were added to fix the piping at the blowers and reduce pipe strain on the blower nozzles.

7. Ambient alignment targets were determined based on Permalign measurements.

References:

1. Atra-Flex Flexible Couplings; http://www.atra-flex.com/

2. ME'scopeVES; http://www.vibetech.com/

3. http://rodyn-inc.com/html_aboutRodyn.html

4. DyRoBeS Software; http://www.dyrobes.com/

5. Bennett, Edward, D'Orsi, Nicholas, Japikse, David, Karon, David, Osborne, Colin; **A Lexicon Of Turbmachinery Performance**, Concepts ETI, Inc., Wilder Vermont, Oct 28-Nov 1, 1991, page 1-15, 1-16.

6. Flexicraft Industries; Metal Expansion Joint Instructions, http://www.flexicraft.com/Metal_Expansion_Joints/

7. Permalign: http://www.ludeca.com/prod_permalign.php